Preparation, spectral characteristics and photolytic stability of anthracene-hindered amine probes: influence of the medium

Pavol Hrdlovič*, Martin Danko, Štefan Chmela

Polymer Institute, Slovak Academy of Sciences, Dúbravská cesta 9, 842 36 Bratislava, Slovak Republic

Abstract

New probes, esters of 3-(9-anthracene)propionic acid with 2,2,6,6-tetramethyl-4-hydroxypiperidine and its oxidized and protonized form, were prepared and spectrally characterized. Spectral measurements were performed in solution and in polymer matrices as polyethylene, isotactic polypropylene, polystyrene, polymethyl methacrylate and polyvinylchloride. Absorption spectra of these derivatives were shifted about 10 nm bathochromically in comparison with anthracene. The longest wavelength absorption band of the parent amine (probe **III**) and its derivatives exhibited the fine vibrational structure in solution and in all polymer matrices. Fluorescence spectra of the probes were red-shifted as compared to anthracene. The vibrational structure of this emission is well preserved in all media. Quantum yield of fluorescence of parent amine is slightly higher than anthracene in methanol. The range of values of quantum yield relative to anthracene of parent amine is rather large (0.3–11) in polymer matrices. The lifetime of fluorescence of parent amine is 3.8 ns in methanol and 4.1 ns in cyclohexane but it is larger in polymer matrices. Both quantum yield and lifetime of oxidized form were smaller in comparison with parent amine. The quantities Φ_{NH}/Φ_{NO} and τ_{NH}/τ_{NO} expressing the extent of intramolecular quenching (electronic energy transfer) are low for this type of probes in methanol solution. In all polymer matrices these values are higher (2–7.5) but there are some differences between ratio calculated from quantum yields and from lifetimes. The photolytical stability of the novel probes is low in polymer matrices at 366 nm irradiation. 2,2,6,6-Tetramethylpiperidine structural unit as parent amine or as stable nitroxyl radical does not exhibit any stabilization effect. © 2002 Elsevier Science B.V. All rights reserved.

Keywords: Probe; Anthracene; Hindered amine; Aminoxide; Fluorescence; Polymer Matrices; Quenching

1. Introduction

Multifunctional fluorescence probes combining different structural units are used to monitor photophysical and photochemical processes in different environments. Preferably, spectral parameters, which exhibit strong dependence on medium, are exploited for this purpose. The parameters connected with fluorescence have some advantages as the high sensitivity, simple detection, easy quantitative evaluation for selected chromophores and large and specific effect of the environment. Simple chromophores as aromatic hydrocarbons or several dyes are not suitable for monitoring several parameters. For that reason, usually more complex molecules containing different structural units—modules—are needed [1].

Free radicals of *N*-oxyl type (aminoxides) derived from 2,2,6,6-tetramethylpiperidine (TEMPO) are used as a suitable structural unit in the more complex probes because

they influence the photophysical and photochemical processes due to paramagnetic effect or electron transfer [2–7]. Intermolecular quenching of singlet and triplet states of aromatic hydrocarbons and ketones was studied in detail [8–17].

Probes containing structural units as 1-naphthoic, 1-naphthylacetic [18], 4-(1-pyrene)butyric acids [19], 1,8-naphthaleneimide [20], 1-pyrenecarboxylic acid, 1-pyreneacetic acid, 4-oxo-4-(1-pyrene)butanoic acid [21] and 2,2,6,6-tetramethyl-4-hydroxypiperidine were prepared and spectrally characterized in solutions and in polymer matrices.

Study of absorption, steady-state and time-resolved fluorescence spectra of adducts of naphthalene chromophore/nitroxyl radical leads to conclusion that the intramolecular quenching involves the opening of the pre-existing radiationless channel in the luminophore [4,18]. On the other hand, the efficient electron transfer taking place after photoinitiation was clearly demonstrated in the simple systems containing 1,4,5,8-naphthalenediimide [6] and in the larger rod-like complex molecules containing 4-amino-1,8-naphthaleneimide as well [22].

* Corresponding author. Tel.: +421-754-773-448;
fax: +421-754-775-923.
E-mail address: upolhrdl@savba.sk (P. Hrdlovič).

In fluorescence probes, which are prepared by linking aromatic hydrocarbon as chromophore with a free radical center of the *N*-oxyl type, formation of excited states and their decay is connected with switching off or on the chromophore emission as a result of intramolecular quenching [2–7,17–21].

The mechanism of inter- or intramolecular quenching of excited singlet or triplet states by *N*-oxyls is not unequivocally established. The following processes are to be considered: (i) catalytic enhancement of intersystem crossing as a result of an increase in spin-orbital coupling due to the paramagnetic effect; (ii) catalytic enhancement of the efficiency of internal conversion; (iii) transfer of electronic energy of resonance or exchange type; (iv) transfer of electron and formation of cation or anion radical. The majority of mechanistic studies of quenching of the singlet state of aromatic hydrocarbons with *N*-oxyl radicals concluded that enhancement of intersystem crossing is the most probable route for dissipation of energy [8–17]. Intermolecular quenching of a triplet state occurs through internal conversion [23].

The photophysical process is a preferred route for deactivation of excited singlet state by intramolecular quenching as well [2,3,7,18,19]. On the other hand, the photoinitiated intramolecular electron transfer from *N*-oxyl to diimide under formation of diimide monoanion was observed [6].

The mechanism of intramolecular quenching of triplet states of aromatic hydrocarbons by *N*-oxyls indicates that mainly photophysical routes are involved [23] but recent triplet quenching of 1,8-naphthaleneimide chromophore monitored by laser flash photolysis points out on electron transfer as well [24,25].

These studies indicate that *N*-oxyl radical is able to quench the excited state by different mechanisms depending on the structure of the couple quenchee–quencher and medium.

There is growing interest to develop multifunctional spin system with synergic properties. Especially, the photofunctional organo-magnetic materials are of great importance because of large versatility of organic compounds. Recently, 1-oxo-2,2,6,6-tetramethyl-4-(9-anthrylmethylamino)piperidine and its photodimer have been prepared to show ferromagnetic interactions in the former radical and the variable spin–spin interactions depending on the solvent molecules incorporated in the crystals in the latter biradical [26].

In this paper we report on synthesis and spectral properties of probe combining aromatic hydrocarbon—anthracene—with parent 2,2,6,6-tetramethyl-4-hydroxypiperidine and its oxidized and protonated form. The spectral properties of different forms of this probe are compared in different polymer matrices since probes, which are suitable for monitoring various parameters in the solid phase, are highly desired. The effect of paramagnetic center on photochemical and photophysical processes will be examined.

2. Experimental

The structures of multifunctional fluorescent probes under study are shown in Scheme 1. The details of the synthesis are given below.

*3-(9-Anthryl)-propionic acid (**I**).* It was prepared following the procedure in [27]. In a 1 l three necked flask equipped with a dropping funnel, condenser and mercury-sealed stirrer, potassium (4.88 g, 0.125 mol) in 200 ml of dry *t*-butyl alcohol was dissolved under Ar atmosphere. A suspension of anthrone (19.4 g, 0.1 mol) in 10 ml of *t*-butyl alcohol was added and the solution was stirred for 1 h at room temperature. To this reddish-brown solution of potassium anthranolate a solution of 7.3 ml (0.11 mol) of acrylonitrile in *t*-butyl alcohol (40 ml) was added dropwise over a period of 1 h. During the addition a bright red precipitate was separated. The reaction mixture was refluxed for 2 h. After the addition of hydrochloric acid (11 ml) in water (225 ml), *t*-butyl alcohol was removed by distillation during which additional water (100 ml) was added. After the removal of 300 ml of distillate, the content in the flask was cooled and the aqueous layer was separated from the brown oil by decantation. The oily nitrile was refluxed for 2 h with 100 ml of concentrated hydrochloric acid. The precipitate was filtered and washed with 100 ml of water. The solid was dissolved in solution of ammonium hydroxide (360 ml) in water (240 ml) and the resulting solution was heated at 100 °C for 4 h with zinc dust (60 g, activated with 6 ml of 3 M $CuSO_4 \cdot 5H_2O$). During the reduction the solution changed color from reddish-orange to pale yellow. The cooled reaction mixture was filtered, extracted with ether and the aqueous layer was acidified with hydrochloric acid. The separated oil was solidified on standing. The crude product (12.64 g, 50%) with m.p. 170–193 °C was crystallized from glacial acetic acid. After washing the crystals with methanol the yield was 8.07 g (33%) of pale yellow crystals with m.p. 192.5–194 °C (Ref. [26] 194–195 °C). ^{1}H NMR ($CDCl_3$) δ: 2.06 (s, 1H, COOH), 2.76–2.81 (m, 2H, –CH$_2$–Ar), 3.9–3.96 (m, 2H, –CH$_2$–CO), 7.18–7.51 (m, 4H, H-2,3,6,7 anthracene), 7.94–7.97 (m, 2H, H-4,5 anthracene), 8.19–8.22 (m, 2H, H-1,8 anthracene), 8.32 ppm (s, 1H, H-10 anthracene). FT-IR (KBr): ν(C=O) 1700 cm^{-1}, ν(anthracene) 735 cm^{-1}.

*Methyl-3-(9-anthryl)-propanoate (**II**).* It was prepared following the procedure in [28]. The solution of **I** (7 g, 0.028 mol) in methanol (5.7 ml, 0.14 mol) and concentrated sulfuric acid (0.4 ml) was refluxed for 7 h. After distillation off methanol, water (50 ml) was added to the rest oil. Product was extracted with ether (3 × 50 ml) and organic solution was washed with water solution of Na_2CO_3 (3 × 50 ml), then with water (2 × 20 ml) and dried over Na_2SO_4. The crude product was crystallized from methanol to yield 6.59 g (89.1%) yellow crystals of methyl ester with m.p. 65–66 °C (Ref. [29] 75–76 °C). ^{1}H NMR ($CDCl_3$) δ: 2.76–2.81 (m, 2H, –CH$_2$–Ar), 3.74 (s, 3H, CH$_3$–O), 3.94–4.0 (m, 2H, CH$_2$–CO), 7.44–7.56 (m, 4H, H-2,3,6,7 anthracene), 8.0–8.03 (d, 2H, H-4,5 anthracene), 8.25–8.28
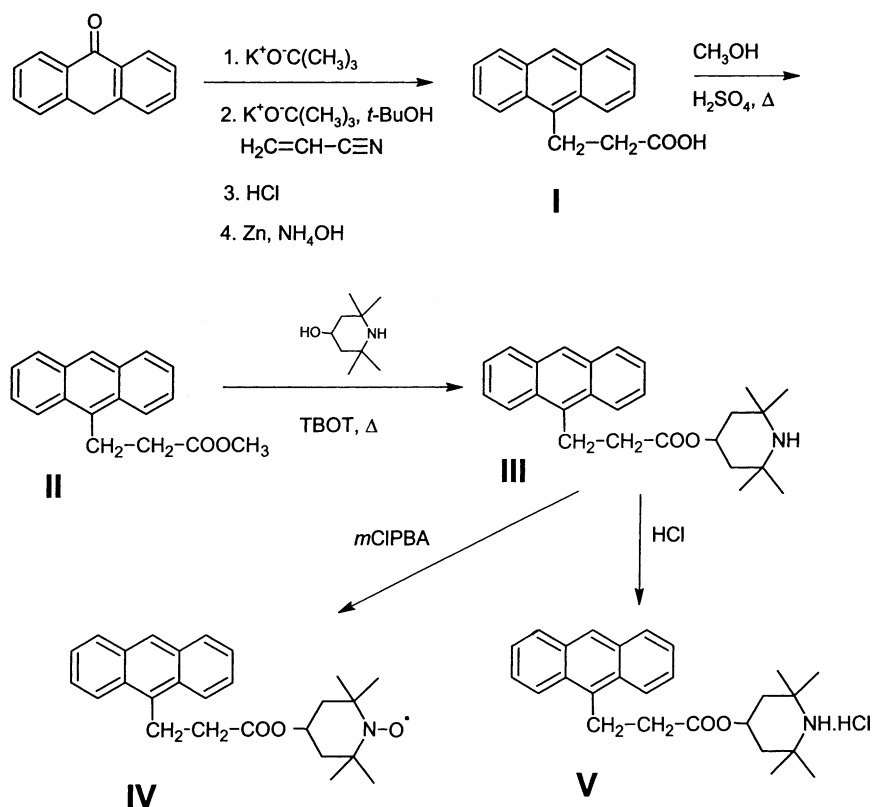
Scheme 1.

(d, 2H, H-1,8 anthracene), 8.37 ppm (s, 1H, H-10 anthracene). FT-IR (KBr): ν(C=O) 1730 cm^{-1}, ν(C–O–C) 1167 cm^{-1}, ν(anthracene) 735 cm^{-1}.

2,2,6,6-Tetramethyl-4-piperidinyl-3-(9-anthryl)-propanoate (III). It was prepared following the procedures described in [18,30]. A solution of **II** (5.5 g, 0.021 mol) and 2,2,6,6-tetramethyl-4-piperidinol (4.875 g, 0.031 mol) in dry xylene was refluxed in presence of tetra-*n*-butylorthotitanate (TBOT, three drops) as re-esterification catalyst for 20 h. In order to shift the equilibrium the alcohol (4 g) and the catalyst (three drops) was added additionally. After evaporation of xylene, the oily product was diluted in ether and precipitated TBOT was filtered. After evaporation of ether, the product was twice crystallized from *n*-hexane to yield 6.164 g (81%) of parent amine with m.p. 91–93 °C. ^{1}H NMR (CDCl$_3$) δ: 1.03–1.11 (m, 2H, CH$_2$, 5 + 3 axial), 1.14 (s, 6H, 2CH$_3$, 2 + 6 axial) 1.24 (s, 6H, 2CH$_3$, 2 + 6 equat.), 1.82–1.88 (m, 2H, CH$_2$, 5 + 3 equat.), 2.73–2.79 (m, 2H, –CH$_2$–Ar), 3.93–3.99 (m, 2H, –CH$_2$–CO), 5.17–5.28 (m, 1H, >CH–O), 7.44–7.55 (m, 4H, H-2,3,6,7 anthracene), 8.0–8.03 (m, 2H, H-4,5 anthracene), 8.25–8.28 (m, 2H, H-1,8 anthracene), 8.37 ppm (s, 1H, H-10 anthracene). FT-IR (KBr): ν(C=O) 1730 cm^{-1}, ν(C–O–C) 1240 cm^{-1}, ν(anthracene) 735 cm^{-1}.

1-Oxo-2,2,6,6-tetramethyl-4-piperidinyl-3-(9-anthryl)-propanoate (IV). It was prepared by oxidation of the parent amine as in [31]. To a solution of **III** (2 g, 0.00515 mol) in 50 ml of dichlomethane *m*-chloroperbenzoic acid (4.447 g, 0.0258 mol) was added per parts at 0 °C under stirring. After 30 min stirring at 0 °C the reaction mixture was heated to room temperature and stirring was continued for 3 h. Then the reaction mixture was cooled to 0 °C and precipitated acid was filtered off. The organic solution was extracted with diluted NaHSO$_4$ (3 × 30 ml) washed with water (2 × 30 ml) and dried with Na$_2$SO$_4$. The product was purified on a column of silica gel (120 g) using ligroin:ethylacetate (10:1) as an eluent. Crystallization from ethanol afforded 0.697 g (30%) of orange crystals with m.p. 125–127 °C. FT-IR (KBr): ν(C=O) 1735 cm^{-1}, ν(C–O–C) 1235 cm^{-1}, ν(anthracene), 735 cm^{-1}.

2,2,6,6-Tetramethyl-4-piperidinyl-3-(9-anthryl)-propanoate hydrochloride (V). It was prepared by bubbling of gaseous hydrochloride through a solution of **III** in mixture of acetone and water (1:1). The precipitated product was filtered, washed with water and dried. Crystallization from methanol yielded white crystals with m.p. > 265 °C. FT-IR (KBr): ν(C=O) 1735 cm^{-1}, ν(C–O–C) 1238 cm^{-1}, ν(anthracene) 735 cm^{-1}, ν(NH$_2$$^+$) 2466 cm^{-1}.

Anthracene (Lachema, Brno, CR) was zonally refined. 1-Oxo-2,2,6,6-tetramethyl-4-hydroxy piperidine was the same as used previously [23]. Solvents: methanol for UV spectroscopy (Slavus, Bratislava, SR), chloroform, dichloromethane, tetrahydrofuran (THF) (Lachema, Brno, CR) analytical grade reagents were used.

Polymers. Polystyrene (PS) (Krasten, Kaucuk Kralupy a.s., CR, SEC (CHCl$_3$) $M_n = 93{,}700$ g mol^{-1}; $M_w/M_n = 2.7$), polymethyl methacrylate (PMMA), (Považské Chemické Závody, Žilina, SR, $M_v = 1.01 \times 10^5$ g mol^{-1}), polyvinyl chloride (PVC), (Neralit 628, Spolana Neratovice, CR, $M_v = 1.11 \times 10^5$ g mol^{-1}) were used. Polymer films doped with probes were prepared by casting on a glass plate (28 mm × 35 mm) of the 1 ml solution of polymers and probe in chloroform or THF (5 g/100 ml). The concentration of probe in polymer films was 0.002 mol kg^{-1}.

Films of low density polyethylene (LDPE, Bralen 2–19, MFI = 1.7–2.3 g/10 min, $d = 0.916$–0.919 g cm^{-3}, Slovnaft, SR) and isotactic polypropylene (iPP, Daplen, PCD Polymere, Schwechat, Austria) were prepared in the following way: The additives (5.95 × 10^{-3} mol kg^{-1}) dissolved in 20 ml of dichloromethane were added to 25 g of non-stabilized polymers powder. The slurry was kept at room temperature for 18 h and then the solvent was removed. The blends were mixed and homogenized in a Brabender Plastograph at 160 °C for LDPE and at 190 °C for iPP for 5 min under air and then hot-pressed in a electrically heated laboratory press (Fontune, The Netherlands) at 160 °C for LDPE and at 200 °C for iPP for 1 min. The thickness of films was 0.08–0.12 mm.

Photolysis (photooxidation) was performed on the merry-go-round type set up. Medium pressure 125 W mercury arc without luminophore envelope (RVL, Tesla Holešovice, CR) was used as the source of radiation in water-cooled quartz reactor. The glass filters (Corning Glass 5860) were used for isolation of 366 nm radiation. The photolysis was performed at laboratory temperature. The course of photolysis was followed by UV spectroscopy monitoring the changes in absorption of anthracene chromophore.

Absorption spectra were taken on a M-40 UV–VIS-spectrometer (C. Zeiss, Jena, FRG), ^{1}H NMR on 300 MHz spectrometer (Bruker, FRG), mass spectra on HP 597 1A (Hewlett Packard, Palo Alto, USA) and FT-IR spectra on Impact 400 (Nicolet, USA). Emission spectra were recorded on a Perkin-Elmer MPF-4 spectrofluorimeter (Perkin-Elmer, Norfolk, CT, USA) which was connected through interface and A/D converter to a microcomputer [32] for data collection, processing and plotting on an *XY* 4110 plotter (Laboratorní pristroje, Prague, CR). Emission of solutions was measured at right angle in a 1 cm cell. The quantum yields were determined relative to anthracene in methanol or cyclohexane. Emission of polymer films was measured in front-face arrangement to the solid sample holder. The quantum yield of polymer films was determined using anthracene as standard and assuming its insensitivity to the medium. The quantum yields in solution and in film were determined according to the relation [33]:

$$\Phi_F = \Phi_F^S \frac{\int_0^\infty I_F(\nu)\, d\nu}{\int_0^\infty I_F^S(\nu)\, d\nu} \left(\frac{1 - 10^{-A^S}}{1 - 10^{-A}} \right)$$

where Φ_F^S is the quantum yield of standard, integrals

$\int_0^\infty I_F(\nu)\, d\nu$ and $\int_0^\infty I_F^S(\nu)\, d\nu$ the areas under curves of the probe and standard, respectively, A and A^S the absorptions of the probe and standard, respectively.

Fluorescence lifetime measurements were performed on an LIF 200 (Lasertechnik, Berlin, Germany), which operates as a stroboscope. The excitation source was a nitrogen laser ($\lambda = 337$ nm) and emission was selected by the use of cut-off filters. The output signal was digitized and transferred to a microcomputer [34]. The fluorescence decay curves were evaluated by simple phase plane method [35] by homemade software [34]. The standard deviation, $G^{1/2} = \sum((I_{exp} - I_{calc})^2/n)^{1/2}$, where I_{exp} and I_{calc} are the experimental and calculated intensities of emission, respectively, was used to judge the quality of fit. It was assumed that decays were mono-exponential if $G^{1/2}$ is <5%. Some measurements were performed on LIF 200 connected to PC using program of J. Snyder 1988 based on [36].

Static and time-resolved fluorescence measurements in solution and in polymer films were performed in the presence of air.

3. Results and discussion

Anthracene derivatives **III–V**, prepared in this study, exhibit spectral properties relatively independent of environment. It is for instance fine structure of the longest wavelength absorption band and fluorescence and other properties, which are relatively independent of environment. In order to use a chromophore as a structural unit of any probe, it should exhibit either strong dependence or relative independence on environment. Especially, the stability of some spectral parameters of the selected chromophore, which is part of the probe, is highly desirable, if the probe should be applied in various environments. The large part of applications of any probe will take place in the solid phase. Therefore, it is reasonable to study the behaviour of new probes in various environments and especially to compare effect of low molecular solvents with those polymer matrices.

The effect of low molecular solvents on spectral properties of compounds of different structure is well understood [37,38]. Less attention was paid to the solvent effect of polymer matrices. In any case understanding of polymer solvent effect is limited [39]. Two extreme cases are to be considered for solvent effect of polymer matrix: (i) polymer matrix is inert even at laboratory temperature, therefore, the same effect as in gaseous phase is to be expected; (ii) polymer matrix exerts the same effect as the low molecular solvents with the same polarity. The real solvent effect of polymer matrix is somewhere between these limiting cases. This picture does not consider the fact that the dynamics of the solvent shell is different for low molecular solvent and polymer matrix.

Anthracene is the chromophore, which exhibits several fluorescence spectral parameters independent of the environment (Fig. 1). This fact will be used to explore the
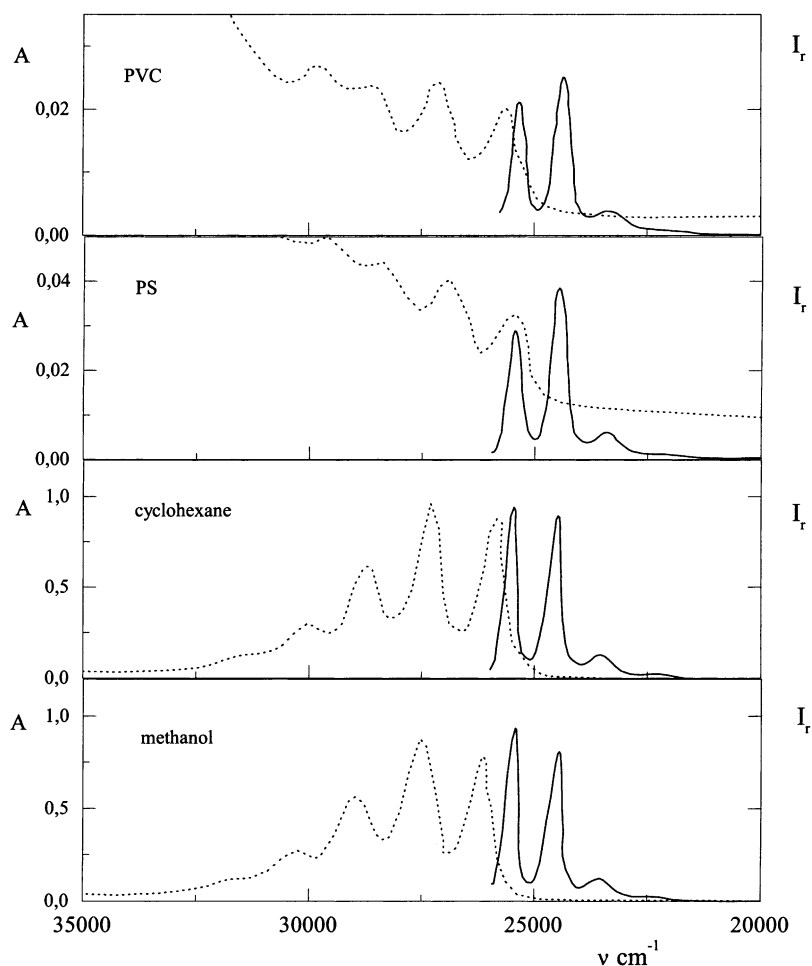
Fig. 1. Absorption (dotted line) and fluorescence (full line) spectra of anthracene in methanol and cyclohexane at 10^{-5} mol dm^{-3}, PVC and PMMA at 0.02 mol kg^{-1}.

medium effect on the intramolecular quenching of fluorophore (derivative of anthracene) by quencher (N-oxyl radical). The typical absorption and emission spectra of parent amine (**III**) are given in Fig. 2 and the relevant spectral data are summarized in Table 1. The spectral data of oxidized (**IV**) and protonized form (**V**) in various environments are given in Tables 2 and 3. The absorption and emission spectra of parent amine (**III**) are red-shifted about 10 nm as compared with anthracene. The longest wavelength band of probes **III**, **IV** and **V** exhibits fine structure in methanol (Tables 1–3). The value of the log ε of the vibrational bands lies in the range 3–4 dm^3 mol^{-1} cm^{-1}. The vibrational structure is preserved in the polymer matrices as well. The values of log ε in polymer matrices are in the same range as in solution but they are loaded with large error due to variation in the thickness and are not given in Tables 1–3.

Fluorescence spectrum of the probe containing parent amine (**III**) in cyclohexane and methanol is bathochromically shifted as compared with anthracene as well. The vibrational structure of fluorescence is distinct and the most intense band in methanol is 0–0 transition. The same

emission spectrum is observed for oxidized and protonized form (Tables 1–3). Basically the same features have spectra of probes under study in polymer matrices. However, the most intense vibrational band of fluorescence in polymer matrices is 0–1 transition. The 0–0 transition in emission spectra of **III** is rather weak in non-polar matrices as PE and iPP but stronger in polar ones. The separation of vibrational bands of absorption as well as fluorescence spectra lies in the range 1500–1300 cm^{-1}. In going from non-polar to polar matrices small red-shift of the most intense band of fluorescence up to 400 cm^{-1} is observed.

Stoke's shift, the difference between 0–0 band of absorption and fluorescence is around 500 cm^{-1} in cyclohexane and methanol and in polymer matrices as well. The small value of Stoke's shift indicates that there is only small difference between the geometry of ground state and excited state and the similar situation is in polymer matrices. The probe **IV** in PE and iPP matrices exhibits the larger values of Stoke's shift.

Quantum yield of fluorescence of **III** and **V** relative to anthracene in methanol is slightly larger than 1 and for **IV**
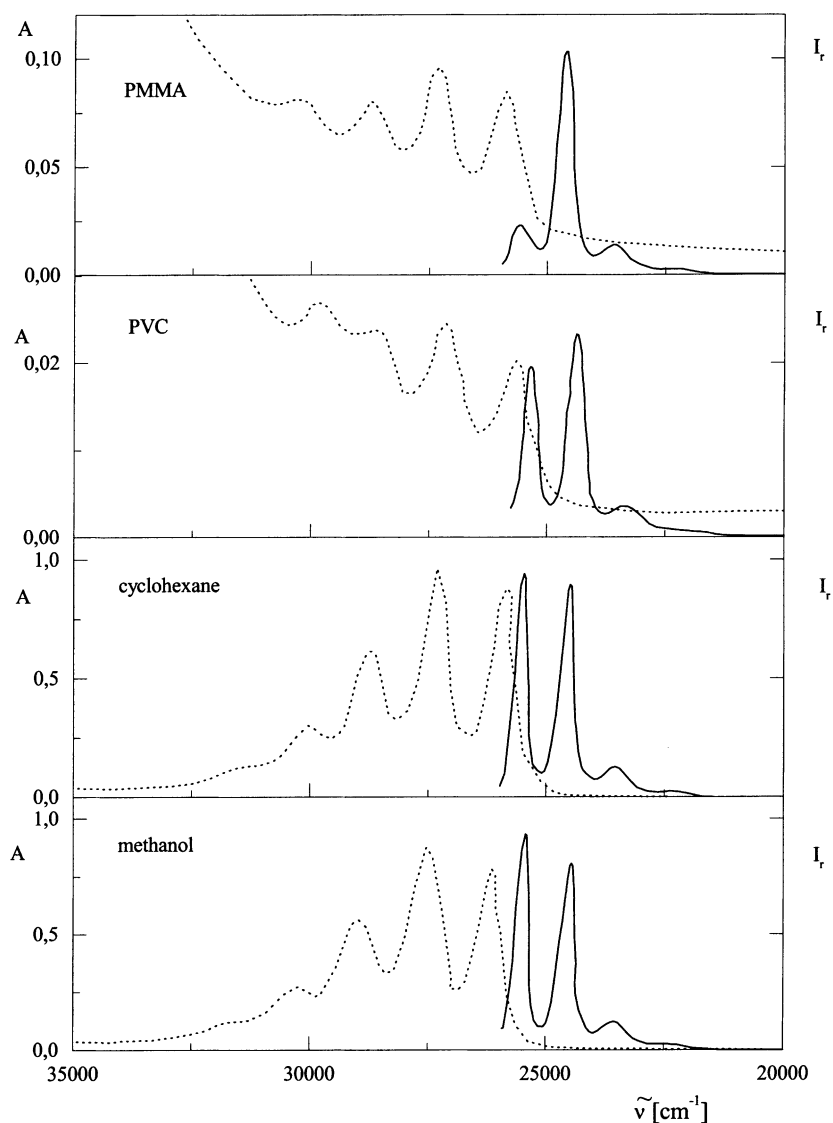
Fig. 2. Absorption (dotted line) and fluorescence (full line) spectra of 2,2,6,6-tetramethyl-4-piperidinyl-3-(9-anthryl)-propanoate (**III**) in methanol and cyclohexane at 10^{-5} mol dm^{-3}, PVC and PMMA at 0.02 mol kg^{-1}.

slightly lower than 1. The relative quantum yields for all probes in polymer matrices lies in the large range 0.1–11. They are rather low in non-polar matrices as PE and iPP (0.1–0.4) but they are increasing in going to more polar PMMA and PVC. This trend with some exceptions is valid for parent amine as well as for nitroxyl radical. The values for nitroxyl radicals are smaller in all cases when compared with the values for parent amine. The large scatter of values of relative quantum yields might be caused that these parameter is inherently loaded with larger error in polymer matrices due to in-homogeneity of the doped probes, variation of the film thickness, and the necessity to measure absorption and emission on the same place with equal geometry of the probing beam. Moreover, the more polar environment decreases the quantum yield of anthracene fluorescence while it increases that of probes **III–V**. This effect

is most pronounced in PVC matrix. Consequently, relative quantum yield as a parameter is loaded with high error and it must be applied with some caution. In spite of this conclusions concerning the intramolecular quenching, based on this parameter seems to be reasonable.

The lifetime of anthracene in degassed cyclohexane is 5.23 and undegassed is 4.1 ns by single photon counting [40]. The lifetime of anthracene, measured on simple set up consisting from nitrogen laser operating as stroboscope, processing the signal by Box Car Integrator and applying the deconvolution by simple phase plane method [34–36], was 3.8 ns. Similar values were measured for probes **III** and **V** in methanol. The lifetime for **IV** was shorter in methanol and all other matrices than that of **III** and **V** with exception of PVC. The standard error of fitting decay curve of **IV** to mono-exponential function was always larger than for **III**

Table 1

Spectral properties of 2,2,6,6-tetramethyl-4-piperidinyl-3-(9-anthryl)-propanoate (**III**) in different media

M^a	ν_{abs}, cm^{-1} (log ε, dm^3 mol^{-1} cm^{-1})^b	ν_{em} $(I_r)^c$ cm^{-1}	$\Phi_r{}^d$	τ^e, ns	$G^{1/2f}$, %	$\Delta\nu^g$, cm^{-1}	$\Phi_{NH}/\Phi_{NO}{}^h$	$\tau_{NH}/\tau_{NO}{}^i$
MeOH	30303 (3.45)	25580 (1.00)	1.2	3.8	1.5	530	1.3	1.2
	28902 (3.79)	24213 (0.86)						
	27624 (3.95)	22883 (0.13)						
	26110 (3.90)	21598 (0.03)						
Cy	30100 (3.45)	25510 (1.00)	0.72	4.1^j		410	4.2	4.2
	28700 (3.79)	24100 (0.95)						
	27300 (3.99)	22900 (0.14)						
	25900 (3.92)	21700 (0.03)						
PE	30030	25130 (0.08)	0.3	6.8	2.7	640	3.0	3.1
	28740	24040 (1.00)						
	27320	22730 (0.14)						
	27770	21410 (0.03)						
iPP	30030	25250 (0.16)	0.4	5.8	3.7	520	2.0	1.7
	28820	24100 (1.00)						
	27170	22780 (0.17)						
	25770	21550 (0.040						
PS	30030	25190 (0.84)	2.2	7.1	4.9	580	3.7	1.8
	28740	24040 (1.00)						
	27100	22573 (0.13)						
	25770	21410 (0.03)						
PPMA	30120	25380 (0.23)	2.4	7.6	2.9	520	2.7	1.9
	28820	23980 (1.00)						
	27320	22730 (0.14)						
	25900	21413 (0.03)						
PVC	29760	25190 (0.87)	11.3	3.9	8.4	380	7.5	>1.0
	28490	23810 (1.00)						
	27030	22570 (0.17)						
	25580	21322 (0.04)						

[a] Medium: MeOH—methanol, Cy—cyclohexane, PE—polyethylene, iPP—isotactic polypropylene, PS—polystyrene, PMMA—polymethyl methacrylate, PVC—polyvinyl chloride.

[b] Maximum of vibrational bands of the lowest wave-number absorption band in cm^{-1} (molar decadic extinction coefficient in dm^3 mol^{-1} cm^{-1}).

[c] Maximum of the vibrational bands of the fluorescence (relative intensity).

[d] Quantum yield relative to anthracene under the same conditions.

[e] Lifetime of the fluorescence determined by phase plane method with home made software [34,35].

[f] Standard error of lifetime.

[g] Stoke's shift.

[h] Efficiency of intramolecular quenching based on relative quantum yields.

[i] Efficiency of intramolecular quenching based on lifetimes.

[j] Lifetime of the fluorescence determined by phase plane method with software of J. Snyder 1988 based on [36].

and **V**, which might be caused by the presence of paramagnetic center. The lifetime of all probes in polar and non-polar polymer matrices is longer than in methanol.

Intermolecular quenching of anthracene and its derivatives (**III–V**) by N-oxyl type quencher occurs with high efficiency (Table 4). The Stern–Volmer plots were linear and knowing lifetime it was possible to determine the bimolecular quenching rate constants, k_q. The values of k_q are slightly above the bimolecular rate constant controlled by diffusion in methanol. The reason for this is not quite clear. Since the Stern–Volmer plots are linear, they do not indicate any ground state complex formation. The quenching was efficient for **IV** as well and no synergism with linked N-oxyl was observed either.

As the value is slightly above 1 for Φ_{NH}/Φ_{NO} and τ_{NH}/τ_{NO} for **III** in methanol (Table 1) it indicates that the intramolecular quenching is not very efficient. The reason is probably rather large separation of chromophore and quencher caused by long link formed by two methylene and carboxyl groups. The position of quenchee and quencher in **IV** is to some extent fixed. It seems to be unfavorable for intramolecular quenching in solution as well as in polymer matrices. Since the intermolecular quenching is effective, the approach of the free N-oxyl radical must probably occur from the other side. The values of Φ_{NH}/Φ_{NO} are larger in polymer matrices showing that the intramolecular quenching is more efficient. This is not unequivocally supported by values of τ_{NH}/τ_{NO}, which are lower than the values of

Table 2
Spectral properties of 1-oxo-2,2,6,6-tetramethyl-4-piperidinyl-3-(9-anthryl)-propanoate (**IV**) in different media

M^a	ν_{abs}, cm^{-1} (log ε, dm^3 mol^{-1} cm^{-1})^b	ν_{em} (I_r)^c, cm^{-1}	Φ_r^d	τ^e, ns	$G^{1/2f}$, %	$\Delta\nu^g$, cm^{-1}
MeOH	30300 (3.18)	25580 (1.00)	0.9	3.2	5.0	390
	28900 (3.78)	24150 (0.82)				
	27470 (3.90)	22880 (0.18)				
	25970 (3.83)	21600 (0.03)				
Cy	30100 (3.32)	25510 (1.00)	0.17	1.0^h		290
	28800 (3.65)	24100 (0.93)				
	27300 (3.86)	22900 (0.15)				
	25800 (3.82)	21500 (0.03)				
PE	30030	24940 (0.15)	0.1	2.2	3.6	970
	28570	24040 (1.00)				
	27400	22830 (0.16)				
	25910	21500 (0.03)				
iPP	30030	25250 (0.11)	0.2	3.5	2.2	660
	28740	24100 (1.00)				
	27170	22830 (0.14)				
	25910	21510 (0.03)				
PS	29760	25190 (0.25)	0.6	3.6	2.8	520
	28490	23870 (1.00)				
	26600	22680 (0.13)				
	25710	21280 (0.03)				
PMMA	30030	25190 (0.12)	0.9	4.0	7.1	580
	28490	24000 (1.00)				
	27100	22680 (0.14)				
	25770	21500 (0.03)				
PVC	29760	25190 (0.35)	1.5	4.2	3.7	580
	28490	23810 (1.00)				
	27030	22570 (0.14)				
	25770	21320 (0.03)				

[a] Medium: MeOH—methanol, Cy—cyclohexane, PE—polyethylene, iPP—isotactic polypropylene, PS—polystyrene, PMMA—polymethyl methacrylate, PVC—polyvinyl chloride.

[b] Maximum of vibrational bands of the lowest wave-number absorption band in cm^{-1} (molar decadic extinction coefficient in dm^3 mol^{-1} cm^{-1}).

[c] Maximum of the vibrational bands of the fluorescence (relative intensity).

[d] Quantum yield relative to anthracene under the same conditions.

[e] Lifetime of the fluorescence determined by phase plane method with home made software [34,35].

[f] Standard error of lifetime.

[g] Stoke's shift.

[h] Lifetime of the fluorescence determined by phase plane method with software of J. Snyder 1988 based on [36].

ratio of relative quantum yields. The largest difference is observed for PVC matrix where static value of Φ_{NH}/Φ_{NO} are large and dynamic value of τ_{NH}/τ_{NO} is even lower than 1. This discrepancy between high ratio Φ_{NH}/Φ_{NO} and low value of τ_{NH}/τ_{NO} in PVC matrix is difficult to explain. On one hand, the high value of Φ_{NH}/Φ_{NO} seems to indicate genuine quenching, while on the other hand, the values of lifetime in PVC seem to be distorted. For other matrices the conditions for intramolecular quenching seem to be more favorable based on Φ_{NH}/Φ_{NO} and τ_{NH}/τ_{NO} data.

Photolysis of anthracene based probes **III** and **IV** in films on air (photooxidation) at 366 nm irradiation occurs with the rate comparable with parent anthracene. The course of this photolysis is monitored by UV spectroscopy by decrease of the longest wavelength absorption band in the region 32,000–27,000 cm^{-1}. The dependence of ln A/A_0 on

time is strongly curved (Fig. 3) and only at the beginning the rate could be estimated (Table 5). The course of photolysis is nearly the same in all matrices. Clearly, there is a rapid oxidation of anthracene moiety although the concentration of oxygen in polymer matrices is rather different (PS 1.64×10^{-3} mol dm^{-3}, PMMA 0.29×10^{-3} mol dm^{-3} and PVC 0.275×10^{-3} mol dm^{-3}) [41]. The oxidation proceeds via endoperoxide formation [42], which is well established. Surprisingly, the presence of sterically hindered amine structural units does not at all inhibit this process. The effect of these probes on the overall stabilization efficiency in the case of photooxidation of isotactic polypropylene is under investigation.

In conclusion one can state that the spectroscopic data obtained on probes **III**–**V** indicate the weak interaction of chromophore and radical center in solutions as well in polymer

Table 3

Spectral properties of 2,2,6,6-tetramethyl-4-piperidinyl-3-(9-anthryl)-propanoate hydrochloride (**V**) in different media

M[a]	ν_{abs}, cm^{-1} (log ε, dm^3 mol^{-1} cm^{-1})[b]	ν_{em} (I_r)[c], cm^{-1}	Φ_r[d]	τ[e], ns	$G^{1/2f}$, %	$\Delta\nu$[g], cm^{-1}
MeOH	30210 (3.24)	25580 (1.00)	1.3	3.8	3.4	330
	28820 (3.65)	23920 (0.83)				
	27400 (3.85)	22880 (0.14)				
	25910 (3.80)	21650 (0.03)				
PS	29940	25190 (0.29)	2.4	9.5	2.7	580
	28490	23810 (1.00)				
	27400	22570 (0.14)				
	25770					
PMMA	30030	25380 (0.14)	1.1	8.5	1.2	390
	28740	23990 (1.00)				
	27100	22730 (0.14)				
	25770	21460 (0.03)				
PVC	30030	25250 (0.36)	10.4	7.4	6.5	460
	28570	23870 (1.00)				
	27030	22570 (0.15)				
	25710	21320 (0.03)				

[a] Medium: MeOH—methanol, PS—polystyrene, PMMA—polymethyl methacrylate, PVC—polyvinyl chloride.
[b] Maximum of vibrational bands of the lowest wave-number absorption band in cm^{-1} (molar decadic extinction coefficient in dm^3 mol^{-1} cm^{-1}).
[c] Maximum of the vibrational bands of the fluorescence (relative intensity).
[d] Quantum yield relative to anthracene under the same conditions.
[e] Lifetime of the fluorescence determined by phase plane method with home made software [34,35].
[f] Standard error of lifetime.
[g] Stoke's shift.

Table 4

Quenching of fluorescence of 3(9-anthryl)propionic acids (**I**) and its derivatives by 1-oxo-2,2,6,6-tetramethyl-4-hydroxypiperidine in methanol

S[a]	K_{SV}[b] (dm^3 mol^{-1})	r[c]	τ[d] (ns)	$G^{1/2e}$ (%)	$k_q \times 10^{-10f}$ (dm^3 mol^{-1} s^{-1})
Anthracene	204 ± 2	0.9982	3.7	1.2	5.5
I	140 ± 4	0.9923	3.7	0.7	3.8
II	125 ± 1	0.9963	3.3	1.7	3.8
III	213 ± 1	0.9986	3.8	1.5	5.6
IV	173 ± 2	0.9963	3.2	5.0	5.6
V	163 ± 2	0.9975	3.8	3.4	4.3

[a] Substrate—quenchee—structure according to Scheme 1.
[b] Stern–Volmer constant.
[c] Correlation coefficient of the Stern–Volmer plot.
[d] Lifetime of fluorescence.
[e] Standard error of lifetime.
[f] Bimolecular rate constant of quenching.

Table 5

The initial rate constant of photooxidation of anthracene derivatives doped in PS, PMMA and PVC films

Probe/matrix[a]	k_A[b] (min^{-1}) PS	k_A[b] (min^{-1}) PMMA	k_A[b] (min^{-1}) PVC
Anthracene	0.021	0.014	0.037
9-Methylanthracene	0.021	0.028	0.009
9,10-Dimethylanthracene	0.024	0.029	0.0124
II	0.026	0.027	0.025
III	0.022	0.038	0.028
IV	0.026	0.042	0.02

[a] Matrices: PS—polystyrene, PMMA—polymethyl methacrylate, PVC—polyvinyl chloride.
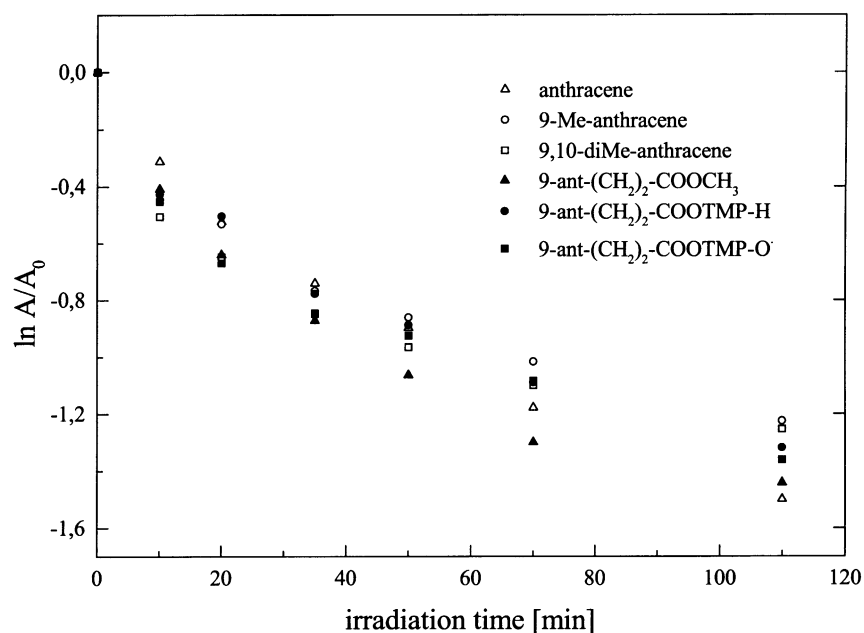[b] The slopes were determined for the initial period of 50 min.

Fig. 3. The course of photooxidation of anthracene based probes by 366 nm irradiation in PS matrix.

matrices. Consequently, the extent of intramolecular quenching is rather low. Moreover the inhibition effect of linked sterically hindered amine on photooxidation of anthracene is rather weak.

Acknowledgements

References

[1] A.P. de Silva, H.Q.N. Gunaratne, T. Gunnlagsson, A.J.M. Huxley, C.P. Mc Coy, J.T. Rademacher, T.E. Rice, Chem. Rev. 97 (1997) 1515.

[2] N.V. Blough, D.J. Simpson, J. Am. Chem. Soc. 110 (1988) 1915.

[3] S.A. Green, D.J. Simpson, G. Zhou, P.S. Ho, N.V. Blough, J. Am. Chem. Soc. 112 (1990) 7337.

[4] J.L. Gerlock, P.J. Zacmanidis, D.R. Bauer, D.J. Simpson, N.V. Blough, I.T. Salmeen, Free Rad. Res. Commun. 10 (1990) 119.

[5] D.J. Kieber, N.V. Blough, Free Rad. Res. Commun. 10 (1990) 109.

[6] S. Green, M.A. Fox, J. Phys. Chem. 99 (1995) 14752.

[7] S.E. Herbelin, N.V. Blough, J. Phys. Chem. B 102 (1998) 8170.

[8] A.R. Watkins, Chem. Phys. Lett. 29 (1974) 526.

[9] A.R. Watkins, Chem. Phys. Lett. 70 (1980) 230.

[10] A.R. Watkins, Chem. Phys. Lett. 70 (1980) 262.

[11] J.C. Scaiano, Chem. Phys. Lett. 79 (1981) 41.

[12] V.A. Kuzmin, A.S. Tatikolov, Chem. Phys. Lett. 51 (1977) 45.

[13] J.A. Green II, L.A. Singer, J. Am. Chem. Soc. 96 (1974) 2730.

[14] S.K. Chattopadhyay, P.K. Das, G.L. Hug, J. Am. Chem. Soc. 105 (1983) 6205.

[15] J. Karpiuk, Z. R Grabowski, Chem. Phys. Lett. 160 (1989) 451.

[16] P. Hrdlovič, J.C. Scaiano, I. Lukáč, J.E. Guillet, Macromolecules 19 (1986) 1637.

[17] T.A. Fayed, G. Grampp, S. Landgraf, Int. J. Photoenergy 1 (1999) 173.

[18] P. Hrdlovič, Š. Chmela, L. Bucsiovč, Chem. Papers 50 (1996) 271.

[19] P. Hrdlovič, Š. Chmela, J. Photochem. Photobiol. A 105 (1997) 83.

[20] P. Hrdlovič, Š. Chmela, M. Danko, J. Photochem. Photobiol. A 112 (1998) 197.

[21] L. Bucsiová, P. Hrdlovič, Š. Chmela, J. Photochem. Photobiol. A 143 (2001) 59.

[22] S.R. Greenfield, W.A. Svec, D. Goszotola, M.R. Wasielewski, J. Am. Chem. Soc. 118 (1996) 6767.

[23] Š. Chmela, P. Hrdlovič, Chem. Papers 38 (1984) 199.

[24] P. Hrdlovič, Š. Chmela, M Sarakha, J. Lacoste J. Photochem. Photobiol. A 138 (2001) 95.

[25] J.E. Rodgers, L.A. Kelly, J. Am. Chem. Soc. 121 (1999) 3854.

[26] T. Okijama, H. Akutsi, J. Yamada, S. Nakatsuji, Chem. Lett. (2000) 918.

[27] G.H. Daub, W.C. Doyle, J. Am. Chem. Soc. 74 (1952) 4449.

[28] Organická Synthesa, Academia Praha, 1971, p. 417.

[29] J.W. Cook, R.S. Ludwiczak, R. Schoental, J. Chem. Soc. (1950) 11120.

[30] P. Hrdlovič, Š. Chmela, L. Horinová, Can. J. Chem. 73 (1995) 1948.

[31] Š. Chmela, M. Danko, P. Hrdlovič, Polym. Degrad. Stabil. 63 (1999) 159.

[32] G. Moyze, J. Mlýnek, D. Jurčák, P. Hrdlovič, Chem. Listy 86 (1992) 57.

[33] A. Kawski, A. Kubicki, B. Kulinski, J. Photochem. Photobiol. A 71 (1993) 161.

[34] D. Jurčák, J. Mlýnek, G. Moyze, P. Hrdlovič, Chem. Listy 83 (1989) 531.

[35] J.N. Demas, A.W. Adamson, J. Phys. Chem. 57 (1971) 2463.

[36] J.N. Demas, Excited State Lifetime Measurements, Appendix E, Academic Press, New York, 1983, p. 245.

[37] P. Suppan, J. Photochem. Photobiol. A 50 (1990) 293.

[38] A. Kawski, in: J.F. Rabek (Ed.), Progress in Photochemistry and Photophysics, Vol. V, CRC Press, Boca Raton, FL, 1992, p. 1 (Chapter 1).

[39] R. Fritz, A. Kungl, W. Rettig, J. Springer, Chem. Phys. Lett. 260 (1996) 409.

[40] R.A. Lampert, L.A. Chewter, D. Phillips, Anal. Chem. 55 (1983) 68.

[41] S. Pauli, in: J. Brandrup, E.H. Immergut (Eds.), Permeability and Diffusion Data, Polymer Handbook, 3rd Edition, Wiley, New York, 1989, p. Vi/435.

[42] J. Aspers, D.J. Carlsson, D.M. Wiles, Macromolecules 9 (1976) 691.